# One-Dimensional Organic–Inorganic Hybrid Perovskite Incorporating Near-Infrared-Absorbing Cyanine Cations

Véron, Anna C ; Linden, Anthony ; Leclaire, Nicolas A ; Roedern, Elsa ; Hu, Shunbo ; Ren, Wei ; Rentsch, Daniel ; Nüesch, Frank A

Abstract: Hybrid perovskite crystals with organic and inorganic structural components are able to combine desirable properties from both classes of materials. Electronic interactions between the anionic inorganic framework and functional organic cations (such as chromophores or semiconductors) can give rise to unusual photophysical properties. Cyanine dyes are a well known class of cationic organic dyes with high extinction coefficients and tunable absorption maxima all over the visible and near-infrared spectrum. Here we present the synthesis and characterization of an original 1D hybrid perovskite composed of NIR-absorbing cyanine cations and polyanionic lead halide chains. This first demonstration of a cyanine-perovskite hybrid material is paving the way to a new class of compounds with great potential for applications in photonic devices.

DOI: https://doi.org/10.1021/acs.jpclett.8b00458

# One-Dimensional Organic-Inorganic Hybrid Perovskite Incorporating Near-Infrared-Absorbing Cyanine Cations



| | |
|---|---|
| Journal: | *The Journal of Physical Chemistry Letters* |
| Manuscript ID | jz-2018-004583.R4 |
| Manuscript Type: | Letter |
| Date Submitted by the Author: | 18-Apr-2018 |
| Complete List of Authors: | Véron, Anna; Swiss Federal Laboratories for Materials Science and Technology (Empa), Laboratory for Functional Polymers; University of Zurich, Department of Chemistry A<br>Linden, Anthony; University of Zurich, Department of Chemistry A<br>Leclaire, Nicolas; Swiss Federal Laboratories for Materials Science and Technology (Empa), Laboratory for Functional Polymers<br>Roedern, Elsa; Empa - Swiss Federal Laboratories for Materials Science and Technology, Materials for Energy Conversion<br>Hu, Shunbo; Shanghai University, Department of Physics<br>Ren, Wei; Department of Physics,<br>Rentsch, Daniel; Empa, Functional Polymers<br>Nüesch, Frank; Empa, Advanced Materials and Surfaces |
| | |

# One-Dimensional Organic-Inorganic Hybrid Perovskite Incorporating Near-Infrared-Absorbing Cyanine Cations

*Anna C. Véron*,[1,2] Anthony Linden,[2] Nicolas A. Leclaire,[1] Elsa Roedern,[1] Shunbo Hu,[3] Wei Ren*,[3] Daniel Rentsch,[1] & Frank A. Nüesch[1,3]*

[1] Empa, Swiss Federal Laboratories for Materials Science and Technology, CH-8600 Dübendorf, Switzerland

[2] Department of Chemistry, University of Zurich, CH-8057 Zurich, Switzerland

[3] Physics Department, Materials Genome Institute, and International Center of Quantum and Molecular Structures, Shanghai University, Shanghai 200444, China

AUTHOR INFORMATION

**Corresponding Author**

*Correspondence should be addressed to A.C.V. (anna.veron@uzh.ch) or W.R. (renwei@shu.edu.cn).

ABSTRACT. Hybrid perovskite crystals with organic and inorganic structural components are able to combine desirable properties from both classes of materials. Electronic interactions between the anionic inorganic framework and functional organic cations (such as chromophores or semiconductors) can give rise to unusual photophysical properties. Cyanine dyes are a well-known class of cationic organic dyes with high extinction coefficients and tunable absorption maxima all over the visible and near-infrared spectrum. Here we present the synthesis and characterization of an original one-dimensional hybrid perovskite composed of NIR-absorbing cyanine cations and polyanionic lead halide chains. This first demonstration of a cyanine-perovskite hybrid material is paving the way to a new class of compounds with great potential for applications in photonic devices.

**TOC GRAPHICS**

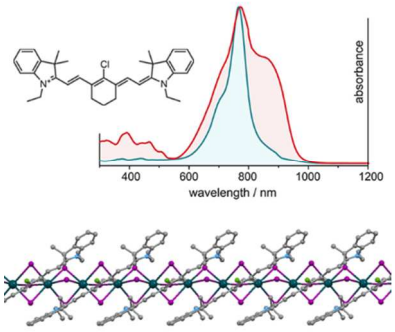

Organic-inorganic hybrid perovskites (OIHPs) are currently receiving tremendous attention due to their exceptional photophysical and electronic properties leading to outstanding performance in, for example, solar cells, and light-emitting devices.[1–3] The most well-known representative of this family of compounds is methylammonium lead iodide ($CH_3NH_3PbI_3$) which adopts a three-dimensional (3D) perovskite crystal structure.[4] Remarkable improvements of perovskite solar cell efficiencies (reaching > 20%) have recently been achieved by fine-tuning the nature of the cations incorporated into the lead halide framework.[5,6] In a 3D perovskite crystal structure, the useable organic cations are strongly limited because of spatial constraints given by Goldschmidt's rule.[7] Specifically for lead halide perovskites, cations must be smaller than ≈ 2.6 Å in diameter in order to fit into the octahedral voids within the inorganic network, which imposes a limit of no more than three non-hydrogen atoms on the organic cations.[8]

When larger organic cations are employed, it is possible to form low-dimensional OIHP structures in which the connectivity of the inorganic network is reduced to two-dimensional (2D) sheets, one-dimensional (1D) chains, or zero-dimensional (0D) clusters.[8–10] Most organic cations in these systems are alkylammonium derivatives with large bandgaps which impact on the properties of the hybrid material indirectly by serving as templating agents, thereby determining the connectivity and spacing of the inorganic construct.[11–14] or by contributing to orientational polarization.[15,16] In contrast to this, there is also the possibility of incorporating functional organic cations which can directly influence the characteristics of the resulting OIHP. Low-bandgap organic chromophores can contribute to the optical properties of the hybrid crystal as strong light absorbers and their molecular orbital levels allow for synergistic interactions with the inorganic component by electron or energy transfer processes. Chromophores investigated for this purpose involve derivatives of tetrathiafulvalene,[17,18] oligothiophene,[19] methylviologen,[20]

tropylium,[21] and naphthalene diimide,[22] which give hybrid materials with interesting features such as semiconducting behavior,[17,18] room temperature photo- and electroluminescence,[19,23] charge-transfer transitions[21,24,25] and panchromatic absorption,[21,22] making these compounds interesting candidates for various photonic applications.[10]

Cyanine dyes are a class of organic chromophores with excellent light-absorbing properties,[26] which have not been explored as ingredients for hybrid perovskites so far. They are well known for their chemical diversity, tunable absorption wavelengths all over the visible and near-infrared (NIR) spectrum and adjustable redox levels.[27] Furthermore, they are iminium cations in their native state and do not require functionalization with cationic moieties, as most other organic chromophores would.

This work presents the synthesis and characterization of an original 1D hybrid perovskite in which NIR-active heptamethine cations are incorporated in an inorganic network of infinite chains of face-sharing lead iodide octahedra. The structure of this compound as its DMF solvate was elucidated using X-ray crystal structure analysis. It was characterized by $^{13}C$ CP-MAS solid state NMR spectroscopy and its light–absorbing properties were evaluated using diffuse reflectance spectroscopy.

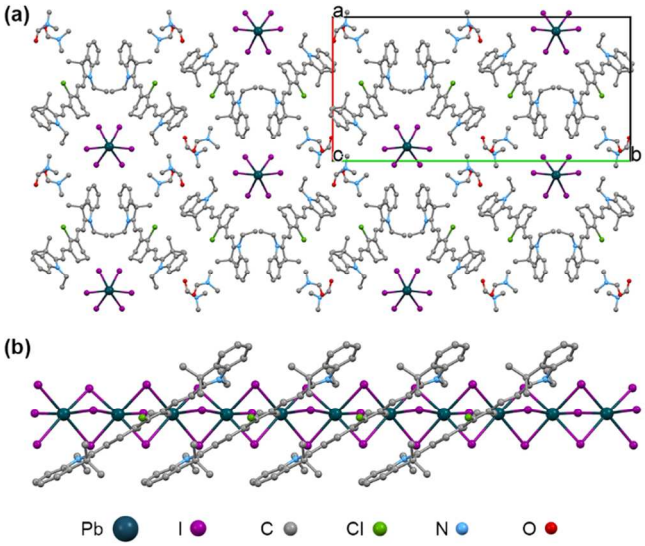


**Figure 1.** Crystal structure packing of $Cy7PbI_3 \cdot 2DMF$. (a) Crystal packing viewed along the c–axis. (b) View of one stack of cyanine cations arranged along a $[PbI_3^-]_n$ chain. Hydrogen atoms omitted for clarity.

$Cy7PbI_3$ was synthesized in 93% yield by layering an acetone solution containing the cyanine iodide salt Cy7I (1.15 eq), $PbI_2$ (1.00 eq), and NaI (1.50 eq) with diethyl ether. The molecular formula of the product ($C_{34}H_{40}ClN_2PbI_3$) was confirmed by elemental analysis. Many procedures for the synthesis of lead halide OIHPs, especially those involving ammonium cations, utilize halic acids both to ensure protonation of the organic amine and to provide an excess of the halide, which is required for the growth of the lead halide network.[21,22] For the synthesis of $Cy7PbI_3$, strongly acidic conditions were avoided to prevent protonation of the cyanine chromophore. Solutions containing only the precursors Cy7I and $PbI_2$ in a 1:1 stoichiometric ratio, however, did not yield any hybrid crystals. Crystallization of the product was found to occur only in the presence of an excess of iodide, which was provided by the addition of NaI.[20] Additionally, the solvate $Cy7PbI_3 \cdot 2DMF$ could be obtained in 60% yield by slow evaporation of

a solution containing Cy7I (1.10 eq), $PbI_2$ (1.00 eq) and NaI (1.00 eq) in DMF, or, in the case of single crystal growth, by the addition of one more equivalent of Cy7I in lieu of the NaI.

X-ray single-crystal structure determination revealed that both precursors co-crystallized into a monoclinic hybrid crystal ($Cy7PbI_3 \cdot 2DMF$) with the general formula $(C_{34}H_{40}ClN_2^+)_n[PbI_3^-]_n \cdot 2n(DMF)$ in the space group $P2_1/c$. The inorganic component forms polyanionic $[PbI_3^-]_n$ chains of face-sharing octahedra running parallel to the c-axis, with the cyanine cations and solvent molecules dispersed between them. The asymmetric unit consists of one cyanine cation $Cy7^+$, one $[PbI_3]^-$ segment of the polyanionic chain and two molecules of DMF (Supporting Information Fig. S1).

The packing of the crystal structure viewed along the c-axis is shown in Fig. 1a. Each $[PbI_3^-]_n$ chain is surrounded by four neighbor columnar stacks of cyanine cations running parallel to the chain and two stacks of DMF molecules. Two of the cation stacks have a side-on approach to an anionic chain and are of themselves inclined in a slightly interpenetrating chevron pattern, while the other two make an end-on approach. Each stack of cations therefore has two anionic chains as nearest neighbors. Within each column of cyanine cations, the interplanar separation of the polymethine planes of adjacent cations is 3.98 Å. The arrangement of one stack of cations along a $[PbI_3^-]_n$ chain is shown in Fig. 1b. Although columnar arrangement of the dye cations in certain cases allows for the formation of spectroscopic *J*-aggregates,[28] closer analysis of the excitonic couplings opposes this assignment as will be explained below.

Unfortunately, the crystal structure of the ansolvate $Cy7PbI_3$ could not be determined, as no suitable crystals could be grown.

Powder X-ray diffraction (PXRD) analysis confirmed that no unreacted precursors Cy7I or $PbI_2$ were present in the product $Cy7PbI_3$ (Fig. 2a–c). The diffraction pattern of the freshly

filtered powder of the solvate $Cy7PbI_3 \cdot 2DMF$ (Fig. 2d) agreed with the simulated pattern derived from the single crystal structure analysis (Supporting Information Fig. S2). After eight hours in air, however, the diffraction pattern of the same sample had changed (Fig. 2e). It showed broad peaks at the same 2θ positions as those obtained in the diffractogram of $Cy7PbI_3$, indicating the loss of DMF and conversion into the solvent-free structure. Also, it was found that after the release of DMF, the residual solid produced a $^{13}C$ CP-MAS NMR spectrum which was identical with that of $Cy7PbI_3$ obtained from acetone/ether (Supporting Information Fig. S5).

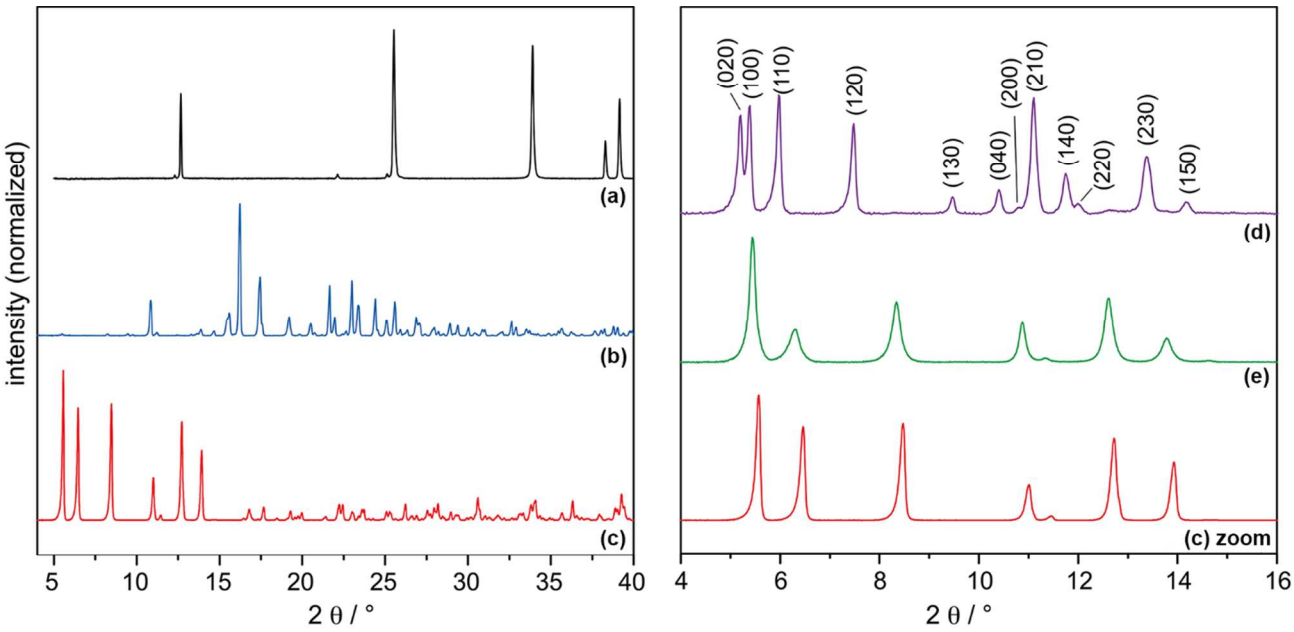


**Figure 2.** Powder X-ray diffraction patterns. (a) $PbI_2$. (b) Cy7I. (c) $Cy7PbI_3$ crystallized from acetone/$Et_2O$. (d) $Cy7PbI_3 \cdot 2DMF$ crystallized from DMF, freshly filtered. (e) Sample d after 8 hours in air at room temperature.

In order to evaluate the optical absorption properties of hybrid compound $Cy7PbI_3$ and its solvate $Cy7PbI_3 \cdot 2DMF$ in comparison with the iodide salt of the cyanine dye Cy7I, the diffuse reflectance spectra of powdered crystalline samples dispersed in a $BaSO_4$ matrix were recorded

and, by applying a remission function, a spectrum proportional to the absorption coefficient was obtained (Fig. 3).

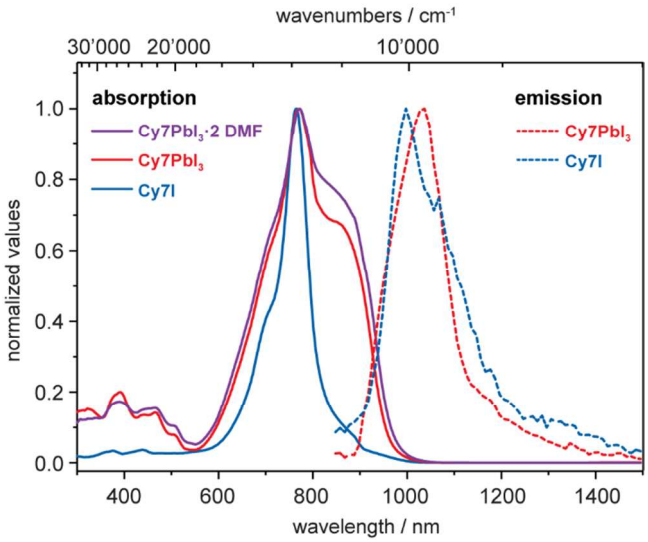


**Figure 3.** Absorption and emission spectra. Solid lines: absorption spectra obtained from diffuse reflectance spectroscopy. The absorption of $Cy7PbI_3$ (red) and its solvate $Cy7PbI_3 \cdot 2DMF$ (purple) is shown in comparison to the iodide salt of the cyanine chromophore Cy7I (blue). Dashed lines: Uncorrected photoluminescence emission spectra obtained at 808 nm laser excitation of $Cy7PbI_3$ (red) and Cy7I (blue) crystalline powders.

The spectrum of pristine Cy7I crystals shows a sharp peak at 766 nm together with a shoulder at 698 nm and 980 nm, respectively. It should be noted, though, that care has to be applied when interpreting diffuse reflectance spectra since braying of organic crystals in $BaSO_4$, may destroy the crystals and manifest monomer like absorption of adsorbates on the reflective matrix. A striking broadening of the spectrum from 820 nm to 1000 nm is observed for the $Cy7PbI_3 \cdot 2DMF$ crystals revealing strong coupling between the chromophores in the crystalline state. Using the extended dipole model, positive exciton coupling energies of $J_{intra}$= 100 $cm^{-1}$ were obtained between adjacent molecules in the stack (Fig. 1b and Fig. S9) meaning that the linear stacks

alone cannot account for the red-shifted absorption band. Instead, it appears that the dominating exciton interaction between translationally non-equivalent molecules in different stacks oriented in a chevron fashion ($J_{inter}$= 216 $cm^{-1}$, Fig. 1a and Fig. S9a) is responsible for the spectral broadening and, in particular, for the red-shifted band. The same features of peak broadening on both the low and high energy side of the monomer peak have been observed for $Cy7PbI_3$, indicating that the ansolvate presents similar chromophore packing. A considerably weaker exciton interaction is obtained for Cy7I crystals ($J_{intra}$= 116 $cm^{-1}$, $J_{inter}$= 105 $cm^{-1}$, Fig. S9b), corroborating smaller absorption bandwidth with respect to $Cy7PbI_3$. The lower intensity features of $Cy7PbI_3 \cdot 2DMF$ and $Cy7PbI_3$ in the UV and visible range from 300 nm to 520 nm comprise contributions from both iodoplumbate and the cyanine chromophore. The main band at 400 nm has been clearly identified as the lowest energy excitonic peak of the one-dimensional $[PbI_3^-]_n$ chain,[29,30] while the absorption features at shorter wavelength have been assigned to direct band-to-band transitions.[25] Interestingly, there are further absorption bands above 400 nm that cannot directly be attributed to the iodoplumbate chain, nor to the pure cyanine solid. In other hybrid crystals with one-dimensional $[PbI_3^-]_n$ chains and high-bandgap conjugated organic cations, charge transfer transitions from the inorganic semiconductor to the organic cation were proposed to explain absorption features at wavelengths above the exciton band at 400 nm.[25,31]

The photoluminescence spectra (PL) of the $Cy7PbI_3$ and Cy7I crystalline powders were recorded using 808 nm laser excitation and right-angle detection and the emission spectra are given in Fig. 3. Both samples showed NIR light emission in the 900–1500 nm spectral region. The hybrid crystals showed an emission peak at 1035 nm with a bandwidth at half maximum (FWHM) of about 1300 $cm^{-1}$ and a rather featureless spectrum. On the other hand, the PL of Cy7I crystals peaked at a shorter wavelength of 1000 nm and presented vibronic shoulders as

well as a larger FWHM of 1520 $cm^{-1}$. The clear differences observed in the PL are related to the molecular packing of the chromophores, thus leading to marked differences in coupling.

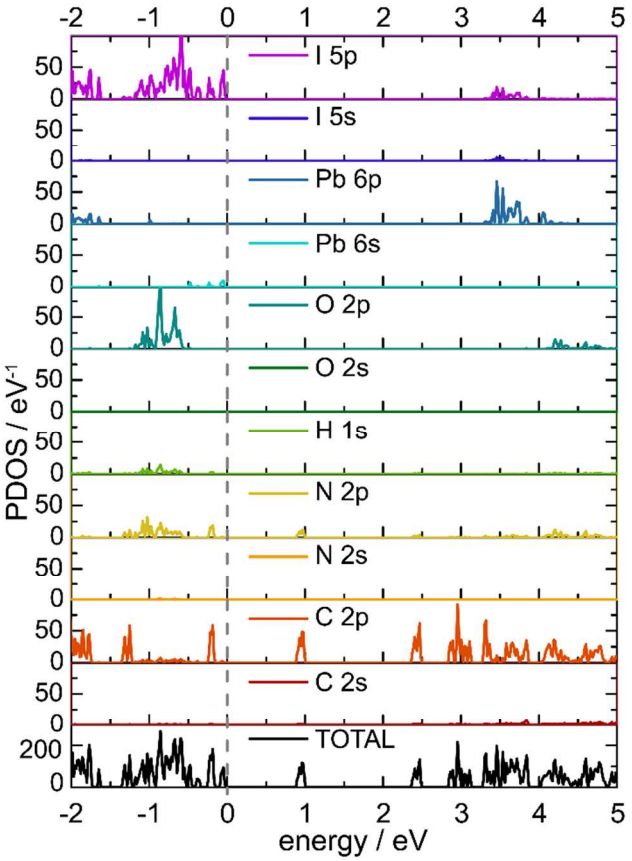


**Figure 4.** Density of States (DOS) of the hybrid perovskite crystal calculated by density functional theory. The total DOS as well as the partial DOS (PDOS) for different orbital contributions are given, and the Fermi level is indicated by a vertical dashed line.

In order to test the hypothesis of charge transfer, electronic structure calculations were carried out using density functional calculations (DFT) with the PBEsol exchange-correlation functional, as implemented in the Vienna Ab initio Simulation Package (VASP),[32,33] and all atoms of the unit cell of the crystal structure (420 atoms). Figure 4 displays the calculated density of states (DOS) decomposed into partial and total density of states. As confirmed by the partial charge density at the band edges (Figure S8), the orbital contribution to the valence band stems

primarily from I5p orbitals of the $[PbI_3^-]_n$ chain, while the conduction band is dominated by C2p orbitals from the chromophore. From Figure 4 it can be inferred that several empty bands with energy higher than the conduction band are based on C2p orbital contributions from the chromophores. The latter may indeed be involved in charge transfer transitions from the iodoplumbate chains to the cyanine chromophore.

In conclusion, organic-inorganic hybrid crystals consisting of one-dimensional iodoplumbate chains and near-infrared absorbing cyanine dye cations have been synthesized and characterized structurally and optically. The latter form one-dimensional molecular stacks with strong exciton coupling of the chromophores within and between the stacks leading to a significantly broadened absorption spectrum in the near infrared domain up to 1000 nm. Due to the low bandgap of the organic semiconductor, several charge transfer bands are observed with transition energies well below the excitonic peak of the $[PbI_3^-]_n$ chains. The latter are corroborated by density functional calculations using the full unit cell contents. These attributes promise interesting photophysical processes[34] with applications in photo refractivity, non-linear optics and optoelectronics.[35] Two possible implementations of such a hybrid material may be put forward to substantiate optoelectronic applications. Light-emitting devices may benefit from high charge mobility in the inorganic chains, while light emission from the organic chromophores occurs via energy transfer from the $[PbI_3^-]_n$ chains to the cyanine stacks. Photodiodes based on photoinduced charge transfer between inorganic chains and organic stacks could be used in detectors. Photoconductivity would be driven by high mobility carriers in the lead iodide chains while the choice of organic dyes incorporated in the hybrid structure would allow tunable spectral sensitivity.

ASSOCIATED CONTENT

**Supporting Information**.

Experimental details and Supporting Figures (PDF),

Crystallographic data for **Cy7PbI$_3$·2DMF** (SG1602.cif),

NMR raw data (Cy7PbI3_NMR raw data.zip).

## AUTHOR INFORMATION

### Notes

The authors declare no competing financial interests.

## ACKNOWLEDGMENT

We thank Beatrice Fischer for IR spectroscopy measurements. Further, we thank Romain Carron, Arndt Remhof, Maksym Kovalenko and Sergii Yakunin for their assistance with diffuse reflectance, PXRD and PL measurements. The supercomputing services from AM-HPC, the High Performance Computing Center at Shanghai University, and Shanghai Supercomputer Center are acknowledged for computation time. F.N. is grateful to the High-End Foreign Expert Program for supporting the collaboration between ICQMS-SHU and Empa. This work was funded by the PV2050 project of the Swiss National Science Foundation (Grant No. 407040_153976), the National Natural Science Foundation of China (51672171) and the National Key Basic Research Program of China (2015CB921600). The NMR hardware was partially granted by the Swiss National Science Foundation (Grant No. 206021_150638/1).

## REFERENCES

(1) Zhao, Y.; Zhu, K. Organic–inorganic Hybrid Lead Halide Perovskites for Optoelectronic and Electronic Applications. *Chem. Soc. Rev.* **2015**, *45*, 655–689.

(2) Green, M. A.; Ho-Baillie, A.; Snaith, H. J. The Emergence of Perovskite Solar Cells. *Nat. Photonics* **2014**, *8*, 506–514.

(3) Manser, J. S.; Christians, J. A.; Kamat, P. V. Intriguing Optoelectronic Properties of Metal Halide Perovskites. *Chem. Rev.* **2016**, *116*, 12956–13008.

(4) Ong, K. P.; Goh, T. W.; Xu, Q.; Huan, A. Structural Evolution in Methylammonium Lead Iodide $CH_3NH_3PbI_3$. *J. Phys. Chem. A* **2015**, *119*, 11033–11038.

(5) Saliba, M.; Matsui, T.; Seo, J.-Y.; Domanski, K.; Correa-Baena, J.-P.; Nazeeruddin, M. K.; Zakeeruddin, S. M.; Tress, W.; Abate, A.; Hagfeldt, A.; et al. Cesium-Containing Triple Cation Perovskite Solar Cells: Improved Stability, Reproducibility and High Efficiency. *Energy Environ. Sci.* **2016**, *9*, 1989–1997.

(6) Jeon, N. J.; Noh, J. H.; Yang, W. S.; Kim, Y. C.; Ryu, S.; Seo, J.; Seok, S. Il. Compositional Engineering of Perovskite Materials for High-Performance Solar Cells. *Nature* **2015**, *517*, 476–480.

(7) Kieslich, G.; Sun, S.; Cheetham, T. An Extended Tolerance Factor Approach for Organic-Inorganic Perovskites. *Chem. Sci.* **2015**, *6*, 3430–3433.

(8) Mitzi, D. B. Synthesis, Structure, and Properties of Organic-Inorganic Perovskites and Related Materials. *Prog. Inorg. Chem.* **1999**, *48*, 1–121.

(9) Saparov, B.; Mitzi, D. B. Organic-Inorganic Perovskites: Structural Versatility for Functional Materials Design. *Chem. Rev.* **2016**, *116*, 4558–4596.

(10) Ganose, A. M.; Savory, C. N.; Scanlon, D. O. Beyond Methylammonium Lead Iodide: Prospects for the Emergent Field of $ns^2$ Containing Solar Absorbers. *Chem. Commun.* **2017**, *53*, 20–44.

(11) Papavassiliou, G. C. Three- and Low-Dimensional Inorganic Semiconductors. *Prog. Solid State Chem.* **1997**, *25*, 125–270.

(12) Billing, D. G.; Lemmerer, A. Synthesis, Characterization and Phase Transitions of the Inorganic–organic Layered Perovskite-Type Hybrids $[(C_nH_{2n+1}NH_3)_2PbI_4]$(n = 12, 14, 16 and 18). *New J. Chem.* **2008**, *32*, 1736–1746.

(13) Kamminga, M. E.; Fang, H.-H.; Filip, M. R.; Giustino, F.; Baas, J.; Blake, G. R.; Loi, M. A.; Palstra, T. T. M. Confinement Effects in Low-Dimensional Lead Iodide Perovskite Hybrids. *Chem. Mater.* **2016**, *28*, 4554–4562.

(14) Zhu, H.; Trinh, M. T.; Wang, J.; Fu, Y.; Joshi, P. P.; Miyata, K.; Jin, S.; Zhu, X.-Y. Organic Cations Might Not Be Essential to the Remarkable Properties of Band Edge Carriers in Lead Halide Perovskites. *Adv. Mater.* **2017**, *29*, 1603072.

(15) Hu, S.; Gao, H.; Qi, Y.; Tao, Y.; Li, Y.; Reimers, J. R.; Bokdam, M.; Franchini, C.; Di Sante, D.; Stroppa, A.; et al. Dipole Order in Halide Perovskites: Polarization and Rashba Band Splittings. *J. Phys. Chem. C* **2017**, *121*, 23045–23054.

(16) Selig, O.; Sadhanala, A.; Müller, C.; Lovrincic, R.; Chen, Z.; Rezus, Y. L. A.; Frost, J. M.; Jansen, T. L. C.; Bakulin, A. A. Organic Cation Rotation and Immobilization in Pure and Mixed Methylammonium Lead-Halide Perovskites. *J. Am. Chem. Soc.* **2017**, *139*, 4068–4074.

(17) Evans, H. A.; Lehner, A. J.; Labram, J. G.; Fabini, D. H.; Barreda, O.; Smock, S. R.; Wu, G.; Chabinyc, M. L.; Seshadri, R.; Wudl, F. (TTF)$Pb_2I_5$ : A Radical Cation-Stabilized Hybrid Lead Iodide with Synergistic Optoelectronic Signatures. *Chem. Mater.* **2016**, *28*, 3607–3611.

(18) Kondo, K.; Matsubayashi, G.-E.; Tanaka, T.; Yoshioka, H.; Nakatsu, K. Preparation and Properties of Tetrathiafulvalene (ttf) and Tetramethyltetraselenafulvalene Salts of Tin(IV) Halide Anions and X-Ray Crystal Structure of $[ttf]_3[SnCl_6]$. *J. Chem. Soc. Dalt. Trans.* **1984**, *1984*, 379–384.

(19) Mitzi, D. B.; Chondroudis, K.; Kagan, C. R. Design, Structure, and Optical Properties of Organic−Inorganic Perovskites Containing an Oligothiophene Chromophore. *Inorg. Chem.* **1999**, *38*, 6246–6256.

(20) Tang, Z.; Guloy, A. M. A Methylviologen lead(II) Iodide: Novel $[PbI_3^-]_\infty$ Chains with Mixed Octahedral and Trigonal Prismatic Coordination. *J. Am. Chem. Soc.* **1999**, *121*, 452–453.

(21) Maughan, A. E.; Kurzman, J. A.; Neilson, J. R. Hybrid Inorganic–Organic Materials with an Optoelectronically Active Aromatic Cation: $(C_7H_7)_2SnI_6$ and $C_7H_7PbI_3$. *Inorg. Chem.* **2015**, *54*, 370–378.

(22) Liu, J.-J.; Guan, Y.-F.; Jiao, C.; Lin, M.-J.; Huang, C.-C.; Dai, W. A Panchromatic Hybrid Crystal of Iodoplumbate Nanowires and J-Aggregated Naphthalene Diimides with Long-Lived Charge-Separated States. *Dalt. Trans.* **2015**, *44*, 5957–5960.

(23) Chondroudis, K.; Mitzi, D. B. Electroluminescence from an Organic−Inorganic Perovskite Incorporating a Quaterthiophene Dye within Lead Halide Perovskite Layers. *Chem. Mater.* **1999**, *11*, 3028–3030.

(24) Savory, C. N.; Palgrave, R. G.; Bronstein, H.; Scanlon, D. O. Spatial Electron-Hole Separation in a One Dimensional Hybrid Organic–Inorganic Lead Iodide. *Sci. Rep.* **2016**, *6*, 20626.

(25) Fujisawa, J.; Ishihara, T. Charge-Transfer Transitions between Wires and Spacers in an Inorganic-Organic Quasi-One-Dimensional Crystal Methylviologen Lead Iodide. *Phys. Rev. B* **2004**, *70*, 113203.

(26) L. Strekowski. Heterocyclic Polymethine Dyes. *Top. Heterocycl. Chem.* **2008**, *14*, 1–241.

(27) Tyutyulkov, N. *Polymethine Dyes: Structure and Properties*; St. Kliment Ohridski University Press, Sofia, Bulgaria, 1991.

(28) Würthner, F.; Kaiser, T. E.; Saha-Möller, C. R. J-Aggregates: From Serendipitous Discovery to Supramolecular Engineering of Functional Dye Materials. *Angew. Chemie Int. Ed.* **2011**, *50*, 3376–3410.

(29) Papavassiliou, G. C.; Koutselas, I. B. Structural, Optical and Related Properties of Some Natural Three- and Lower-Dimensional Semiconductor Systems. *Synth. Met.* **1995**, *71*, 1713–1714.

(30) Duan, H.-B.; Yu, S.-S.; Liu, S.-X.; Zhang, H. An Inorganic–organic Hybrid Crystal with a Two-Step Dielectric Response and Thermochromic Luminescence. *Dalt. Trans.* **2017**, *46*, 2220–2227.

(31) Wan, K.-M.; Tong, Y.-B.; Li-Li, L.-L.; Zou, Y.; Duan, H.-B.; Liu, J.-L.; Ren, X.-M. Investigation of Thermochromic Photoluminescent, Dielectric and Crystal Structural Properties

for an Inorganic–organic Hybrid Solid of [1-Hexyl-3-methylimidazolium][$PbBr_3$]. *New J. Chem.* **2016**, *40*, 8664–8672.

(32) Kresse, G.; Furthmüller, J. Efficient Iterative Schemes for Ab Initio Total-Energy Calculations Using a Plane-Wave Basis Set. *Phys. Rev. B - Condens. Matter Mater. Phys.* **1996**, *54*, 11169–11186.

(33) Perdew, J. P.; Ruzsinszky, A.; Csonka, G. I.; Vydrov, O. A.; Scuseria, G. E.; Constantin, L. A.; Zhou, X.; Burke, K. Generalized Gradient Approximation for Solids and Their Surfaces. *Phys. Rev. Lett.* **2007**, *100*, 136406.

(34) Agranovich, V. M.; Gartstein, Y. N.; Litinskaya, M. Hybrid Resonant Organic-Inorganic Nanostructures for Optoelectronic Applications. *Chem. Rev.* **2011**, *111*, 5179–5214.

(35) Parola, S.; Julián-López, B.; Carlos, L. D.; Sanchez, C. Optical Properties of Hybrid Organic-Inorganic Materials and Their Applications. *Adv. Funct. Mater.* **2016**, *26*, 6506–6544.

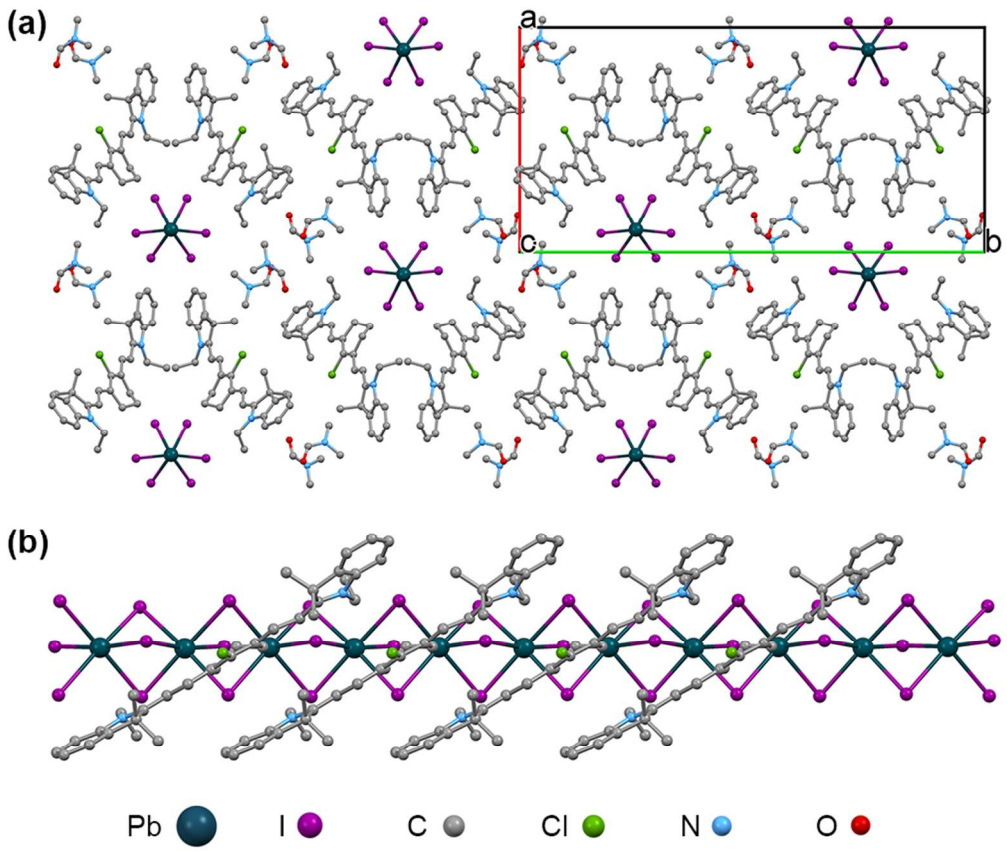


Figure 1. Crystal structure packing of Cy7PbI$_3$·2DMF.‼ ┼ a, Crystal packing viewed along the c–axis. b, view of one stack of cyanine cations arranged along a [PbI$_3$–]n chain. Hydrogen atoms omitted for clarity.

85x71mm (300 x 300 DPI)

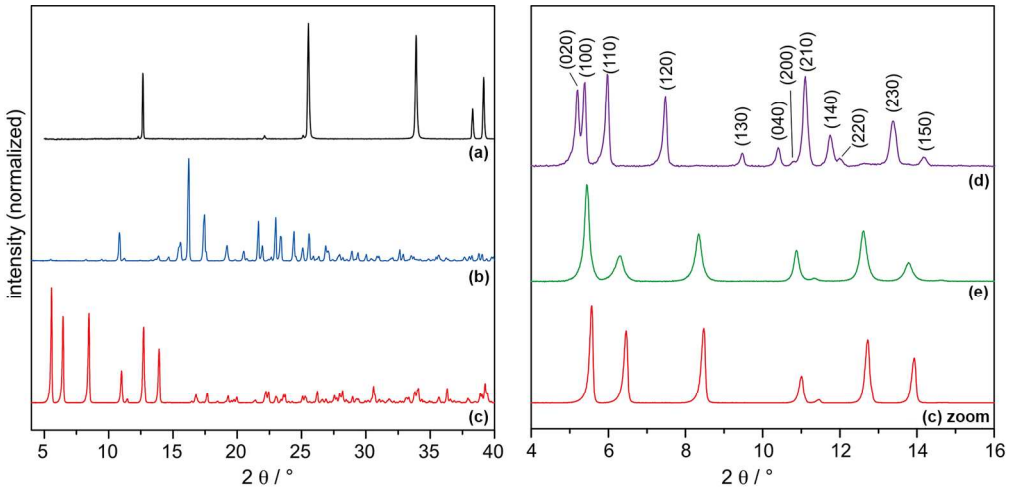


Figure 2. Powder X-ray diffraction patterns. (a) $PbI_2$. (b) Cy7I. (c) $Cy7PbI_3$ crystallized from acetone/$Et_2O$. (d) $Cy7PbI_3 \cdot 2DMF$ crystallized from DMF, freshly filtered. (e) Sample d after 8 hours in air at room temperature.

170x82mm (300 x 300 DPI)

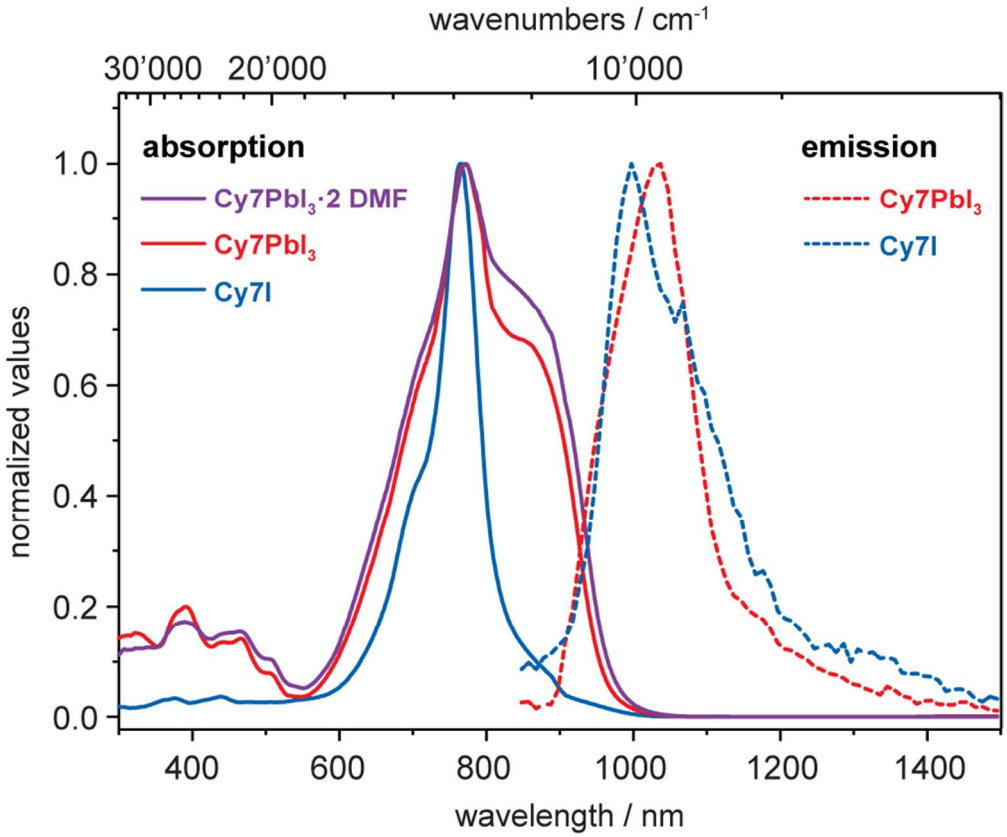


Figure 3. Absorption and emission spectra. Solid lines: absorption spectra obtained from diffuse reflectance spectroscopy. The absorption of Cy7PbI3 (red) and its solvate Cy7PbI3·2DMF (purple) is shown in comparison to the iodide salt of the cyanine chromophore Cy7I (blue). Dashed lines: Uncorrected photoluminescence emission spectra obtained at 808 nm laser excitation of Cy7PbI3 (red) and Cy7I (blue) crystalline powders.

85x71mm (300 x 300 DPI)

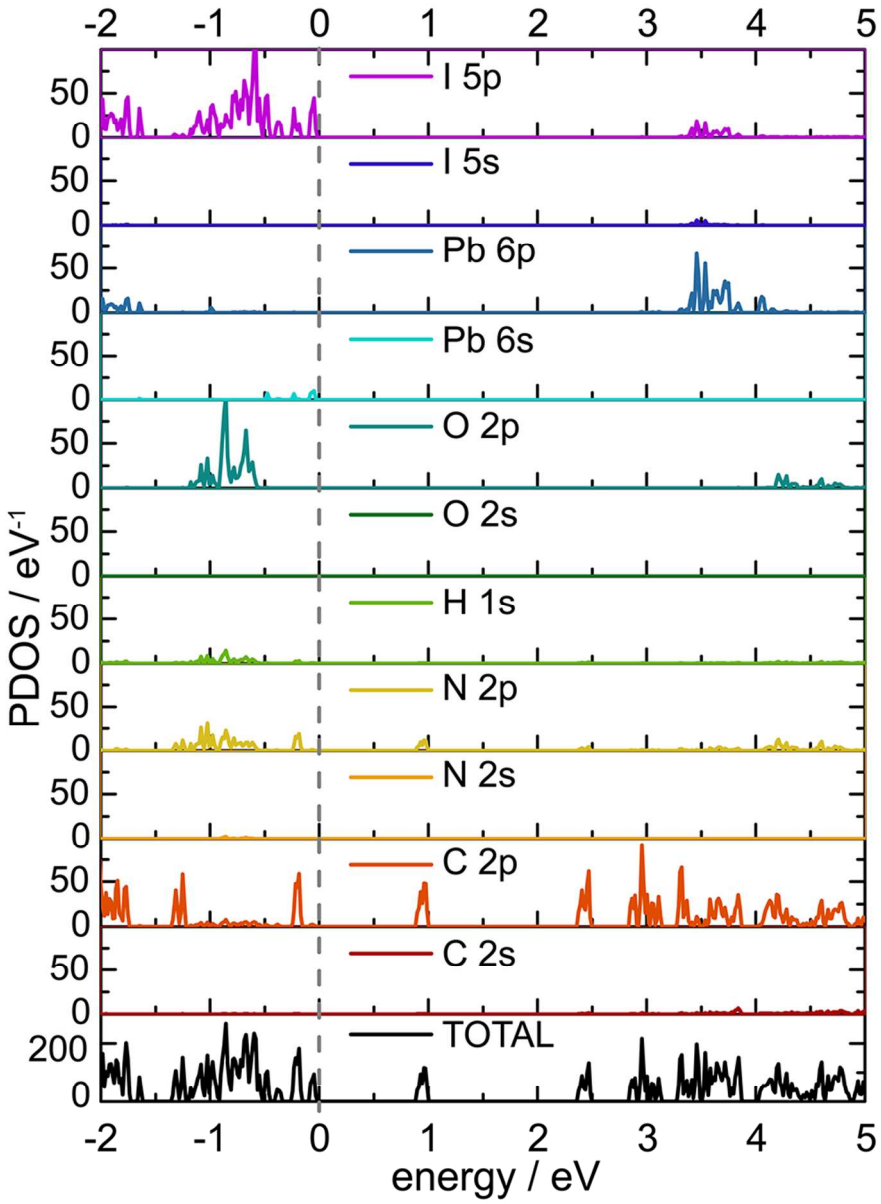


Figure 4. Density of States (DOS) of $Cy7PbI_3 \cdot 2DMF$ calculated by density functional theory. The total DOS as well as the partial DOS (PDOS) for different orbital contributions are given, and the Fermi level is indicated by a vertical dashed line.

85x114mm (300 x 300 DPI)